



# An Experimental Investigation of the Influence of the Lubricant Viscosity and Additives on Gear Wear

Timothy L. Krantz

U.S. Army Research Laboratory, Glenn Research Center, Cleveland, Ohio

Ahmet Kahraman

The Ohio State University, Columbus, Ohio

## The NASA STI Program Office . . . in Profile

Since its founding, NASA has been dedicated to the advancement of aeronautics and space science. The NASA Scientific and Technical Information (STI) Program Office plays a key part in helping NASA maintain this important role.

The NASA STI Program Office is operated by Langley Research Center, the Lead Center for NASA's scientific and technical information. The NASA STI Program Office provides access to the NASA STI Database, the largest collection of aeronautical and space science STI in the world. The Program Office is also NASA's institutional mechanism for disseminating the results of its research and development activities. These results are published by NASA in the NASA STI Report Series, which includes the following report types:

- **TECHNICAL PUBLICATION.** Reports of completed research or a major significant phase of research that present the results of NASA programs and include extensive data or theoretical analysis. Includes compilations of significant scientific and technical data and information deemed to be of continuing reference value. NASA's counterpart of peer-reviewed formal professional papers but has less stringent limitations on manuscript length and extent of graphic presentations.
- **TECHNICAL MEMORANDUM.** Scientific and technical findings that are preliminary or of specialized interest, e.g., quick release reports, working papers, and bibliographies that contain minimal annotation. Does not contain extensive analysis.
- **CONTRACTOR REPORT.** Scientific and technical findings by NASA-sponsored contractors and grantees.

- **CONFERENCE PUBLICATION.** Collected papers from scientific and technical conferences, symposia, seminars, or other meetings sponsored or cosponsored by NASA.
- **SPECIAL PUBLICATION.** Scientific, technical, or historical information from NASA programs, projects, and missions, often concerned with subjects having substantial public interest.
- **TECHNICAL TRANSLATION.** English-language translations of foreign scientific and technical material pertinent to NASA's mission.

Specialized services that complement the STI Program Office's diverse offerings include creating custom thesauri, building customized databases, organizing and publishing research results . . . even providing videos.

For more information about the NASA STI Program Office, see the following:

- Access the NASA STI Program Home Page at <http://www.sti.nasa.gov>
- E-mail your question via the Internet to [help@sti.nasa.gov](mailto:help@sti.nasa.gov)
- Fax your question to the NASA Access Help Desk at 301-621-0134
- Telephone the NASA Access Help Desk at 301-621-0390
- Write to:  
NASA Access Help Desk  
NASA Center for Aerospace Information  
7121 Standard Drive  
Hanover, MD 21076



# An Experimental Investigation of the Influence of the Lubricant Viscosity and Additives on Gear Wear

Timothy L. Krantz

U.S. Army Research Laboratory, Glenn Research Center, Cleveland, Ohio

Ahmet Kahraman

The Ohio State University, Columbus, Ohio

National Aeronautics and  
Space Administration

Glenn Research Center

## Acknowledgments

The authors thank Gurinder Singh for measuring the gear surfaces and for processing the data to determine wear amounts. They also thank M&M Precision Systems, Inc. for making the gear coordinate measurement machine available.

Available from

NASA Center for Aerospace Information  
7121 Standard Drive  
Hanover, MD 21076

National Technical Information Service  
5285 Port Royal Road  
Springfield, VA 22100

Available electronically at <http://gltrs.grc.nasa.gov>

# **An Experimental Investigation of the Influence of the Lubricant Viscosity and Additives on Gear Wear**

Timothy L. Krantz  
U.S. Army Research Laboratory  
Glenn Research Center  
Cleveland, Ohio 44135

Ahmet Kahraman  
The Ohio State University  
Columbus, Ohio 43210

## **Abstract**

The influence of lubricant viscosity and additives on the average wear rate of spur gear pairs was investigated experimentally. The gear specimens of a comprehensive gear durability test program that made use of seven lubricants covering a range of viscosities were examined to measure gear tooth wear. The measured wear was related to the as-manufactured surface roughness, the elastohydrodynamic film thickness, and the experimentally determined contact fatigue lives of the same specimens. In general, the wear rate was found to be inversely proportional to the viscosity of the lubricant and to the lambda ratio (also sometimes called the specific film thickness). The data also show an exponential trend between the average wear rates and the surface fatigue lives. Lubricants with similar viscosities but differing additives and compositions had somewhat differing gear surface fatigue lives and wear rates.

## **1. Introduction**

Surface wear is considered to be one of the important failure modes in gear systems. Gear contact surface wear can significantly impair the functionality of any gear system. Apart from the direct material loss that leads to functional failure, wear can also lead to changes in vibration and noise behavior (refs. 1 to 3). In addition, wear can change the patterns of gear contact such that the altered load distributions and contact stresses will accelerate the occurrence of other failure modes (ref. 4). Therefore, a better understanding of gear wear, including its impact on noise and durability, is needed.

Wear of contacting surfaces is a complex phenomenon that is influenced by a large number of parameters. Gear wear is further complicated since the mechanics of the contact are dictated not only by the geometry but also by both tooth contact and tooth bending deformations. In addition, many automotive and aerospace gearing applications operate in mixed elastohydrodynamic (EHD) or boundary lubrication regimes where asperity contacts are possible (ref. 5). Hence, parameters influencing the lubricant film and boundary layer properties are also critical. The strong coupling between the actual geometries of the worn contacting surfaces and the resulting contact conditions is often ignored in widely used models to estimate stresses and surface fatigue life. Such a simplified approach can perhaps provide unrealistic life predictions.

The study of wear is becoming one of the emerging areas of gear research. A number of recent wear modeling efforts (refs. 6 to 10) form a solid foundation for studying gear wear. The common thread to these studies is that almost all of them use the well-known Archard's wear model (ref. 11) in conjunction with a gear contact model and relative sliding calculations. Archard's wear equation can be expressed for a local point on one of the contacting gear surfaces as

$$\frac{dh}{ds} = kP \quad (1)$$

where  $k$  is an experimentally determined wear coefficient,  $h$  is the wear depth accumulated,  $P$  is the contact pressure, and  $s$  is the sliding distance between the mating surfaces at the point of interest. From equation (1) to calculate the wear depth  $h$ , the contact pressure  $P$  and the sliding distance  $s$  must be determined. Flodin and Andersson (refs. 7 to 9) and Bajpai et al. (ref. 10) proposed wear models for spur and helical gears, and the focus was to determine  $P$  and  $s$ . The tooth contact pressures  $P$  were computed in these models using either simplified Hertzian contact (refs. 7 through 9) or boundary element (ref. 10) formulations under quasi-static conditions. Sliding distance  $s$  calculations were determined from gearing kinematics, and Archard's wear model (ref. 11) was used with an empirical wear coefficient to compute the surface wear distribution.

Perhaps the most significant shortcoming of these models is that they consider wear depth to be a function of only two parameters, contact pressure,  $P$  and sliding distance,  $s$ . All other influences, such as surface material, surface roughness and lubrication at the contact interface, are all accounted for by the wear coefficient  $k$  (ref. 12). When all of the parameters including lubricant type, temperature, flow rate, gear material composition, surface topography, and surface hardness are consistent, then it is possible to define  $k$  using a small number of controlled experiments (ref. 10). However, if all of the stated properties are not consistent, then determining a wear rate coefficient might become a challenging task. In addition, the influence of such parameters on wear cannot be described by these models.

The main objective of this study is to investigate the influence of lubricant viscosity and additives on the wear rate of spur gear pairs. It is the intention of this study to demonstrate experimentally that the lubricant viscosity influences the wear characteristics of gears significantly. The gear specimens of a comprehensive gear durability test program, using seven lubricants covering a range of viscosity, are examined to measure gear tooth surface wear. Wear rates are related to the lubrication conditions (lambda ratios) and the resultant contact fatigue lives of the same specimens. This study is provided to help guide future efforts such that gear wear could be modeled in a more general manner including direct consideration of the lubricant properties and lubrication conditions.

## 2. Test Methodology

### 2.1 Background

The gear experiments of this study were conducted by Townsend and Shimski (ref. 13). The purpose of the experiments was to investigate the influence of lubricant viscosity and additives on gear surface fatigue lives. The comprehensive test program demonstrated and quantified the increase in gear surface fatigue life owing to increased lubricant viscosity. Test specimens and test records were available for further inspection and analysis for the present study of gear wear. The test apparatus, specimens, lubricants, and procedures were reported by Townsend and Shimski (ref. 13). The information needed to document the present research is repeated herein for completeness.

### 2.2 Test Apparatus

The gear fatigue tests were performed in the NASA Glenn Research Center's gear test apparatus. The test rig is shown in figure 1 and described in reference 14. The rig uses the four-square principle of applying test loads, and thus the input drive only needs to overcome the frictional losses in the system. The test rig is belt driven by a variable speed electric motor. All tests reported herein were conducted at a constant speed of 10,000 rpm. Four tests rigs were used and operated 24 hours a day to provide for the large numbers of test cycles required for surface fatigue testing.

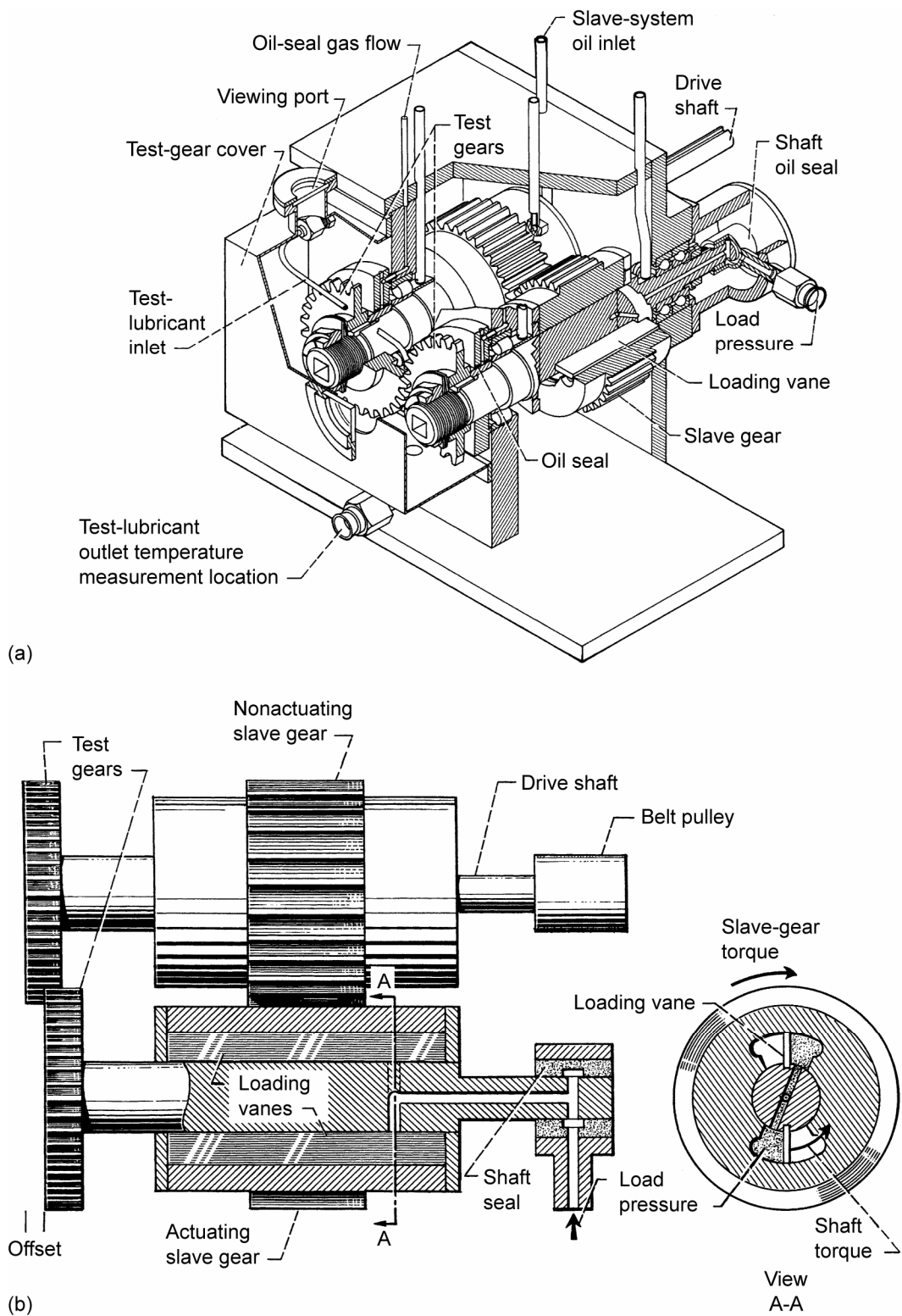


Figure 1.—NASA Glenn Research Center gear fatigue test apparatus. (a) Cutaway view. (b) Schematic view.

The loads on the test gears are provided using hydraulic pressure. A schematic of the apparatus is shown in figure 1(b). Oil pressure and leakage replacement flow is supplied to the load vanes through a shaft seal. As the oil pressure is increased on the load vanes located inside one of the slave gears, torque is applied to its shaft. This torque is transmitted through the test gears and back to the slave gears. In this way, power is circulated, and the desired load and corresponding stress level on the test gear teeth may be obtained by adjusting the hydraulic pressure. The two identical test gears may be started under no load, and the load can then be applied gradually. In order to enable testing at the desired contact stress, the gears are tested with the faces offset as shown in figure 1. By utilizing the offset testing arrangement for both faces of the gear teeth, a total of four surface fatigue tests can be run for each pair of gears.

Separate lubrication systems are provided for the test and slave gears. The two lubrication systems are separated at the gearbox shafts by pressurized labyrinth seals, with nitrogen as the seal gas. Inlet and outlet oil temperatures were continuously monitored. Cooled lubricant was supplied to the inlet of the gear mesh at 0.8 liter/min (0.2 gal/min) and  $320 \pm 7$  K ( $116 \pm 13$  °F). The lubricant outlet temperature was recorded and observed to have been maintained at  $348 \pm 4.5$  K ( $166 \pm 8$  °F). The lubricant was circulated through a 5- $\mu$ m- (200- $\mu$ in.-) nominal fiberglass filter to remove wear particles. For each test, 3.8 liter (1 gal) of lubricant was used.

The purpose of tests by Townsend and Shimski (ref. 13) was to measure gear surface fatigue lives. A vibration transducer mounted on the gearbox was used to automatically stop the test rig when gear surface fatigue damage occurred. Surface fatigue damage caused an increase in the broad-band (root-mean-squared magnitude) acceleration. The gearbox is also automatically stopped if there is a loss of oil flow to either the slave gearbox or the test gears, if the test gear oil overheats, or if there is a loss of seal gas pressurization.

### 2.3 Test Specimens

The test gears used for this work were manufactured from a single heat of consumable-electrode vacuum-melted (CVM) AISI 9310 steel. The gears were manufactured in two lots to the same specifications. The nominal chemical composition of the AISI 9310 material is given in table 1. The gears were case carburized and heat treated according to table 2. The nominal properties of the carburized gears were a case hardness of Rockwell C60, a case depth of 0.97 mm (0.038 in.), and a core hardness of Rockwell C38. The measured hardness profile of the gears is provided in figure 2. From figure 2, the hardness profile is considered to have not been changed significantly with running. Examined microstructure and typical residual stress profiles for such test gears have been reported (refs. 14 and 15).

TABLE 1.—NOMINAL CHEMICAL COMPOSITION  
OF AISI 9310 GEAR MATERIAL

Element	Weight %
Carbon	0.10
Nickel	3.22
Chromium	1.21
Molybdenum	0.12
Copper	0.13
Manganese	0.63
Silicon	0.27
Sulfur	0.005
Phosphorous	0.005
Iron	balance



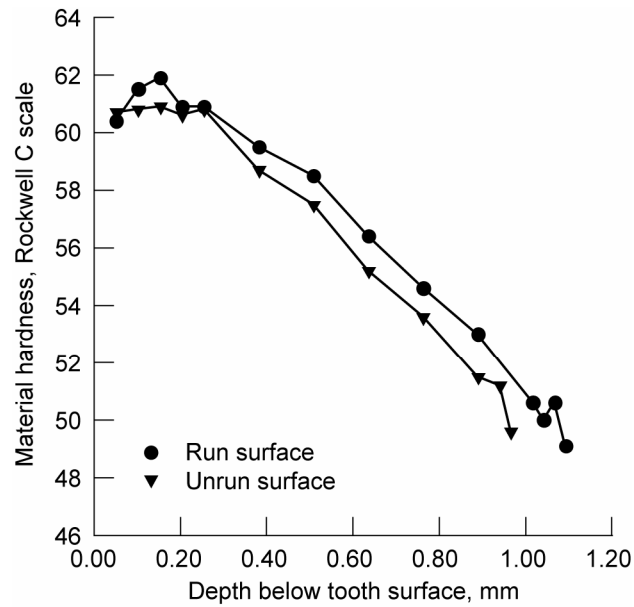


Figure 2.—Measured material hardness versus depth below the pitch-radius surface. Hardness values are converted from Knoop microhardness measurements.

TABLE 2.—HEAT TREATMENT FOR AISI 9310 GEARS

Step	Process	Temperature		Time, hr
		K	°F	
1	Preheat in air	-----	-----	-----
2	Carburize	1,172	1,650	8
3	Air cool to room temperature	-----	-----	-----
4	Copper plate all over	-----	-----	-----
5	Reheat	922	1,200	2.5
6	Air cool to room temperature	-----	-----	-----
7	Austentize	1,117	1,550	2.5
8	Oil quench	-----	-----	-----
9	Subzero cool	180	−120	3.5
10	Double temper	450	350	2 each
11	Finish grind	-----	-----	-----
12	Stress relieve	450	350	2

The dimensions for the test gears are given in table 3. The gear pitch diameter was 89 mm (3.5 in.) and the tooth form was a 20° involute profile modified to provide a tip relief of 0.013 mm (0.0005 in.) starting at the highest point of single tooth contact. The gears have zero lead crowning but do have a nominal 0.13-mm- (0.005-in.-) radius edge break at the tips and sides of the teeth. The gear tooth surface finish after final grinding was specified as a maximum of 0.406  $\mu\text{m}$  (16  $\mu\text{in.}$ ) rms. Tolerances for the gear geometries were specified to meet AGMA (American Gear Manufacturers Association) quality level class 12.

TABLE 3.—SPUR TEST GEAR DESIGN PARAMETERS  
GEAR TOLERANCES ARE PER AGMA CLASS 12

Number of teeth	28
Module, mm	3.175
Diametral pitch (1/in.)	8
Circular pitch, mm (in.)	9.975 (0.3927)
Whole depth, mm (in.)	7.62 (0.300)
Addendum, mm (in.)	3.18 (.125)
Chordal tooth thickness ref. mm (in.)	4.85 (0.191)
Pressure angle, deg.	20
Pitch diameter, mm (in.)	88.90 (3.500)
Outside diameter, mm (in.)	95.25 (3.750)
Root fillet, mm (in.)	1.02 to 1.52 (0.04 to 0.06)
Measurement over pins, mm (in.)	96.03 to 96.30 (3.7807 to 3.7915)
Pin diameter, mm (in.)	5.49 (0.216)
Backlash reference, mm (in.)	0.254 (0.010)
Tip relief, mm (in.)	0.010 to 0.015 (0.0004 to 0.0006)

## 2.4 Test Procedure

The test gears were cleaned to remove the preservative and assembled on the test rig. The test gears were run with the tooth faces offset by 3.3 mm (0.130 in.). All tests were run-in at a load (tangent to the pitch circle) per unit face width of 123 N/mm (700 lb/in.) for one hour. The load was then increased to the test load of 580 N/mm (3300 lb/in.), which resulted in a 1.7 GPa (250 ksi) pitch-line maximum Hertz stress. The Hertz stress just stated is an idealized stress value assuming static equilibrium, perfectly smooth surfaces, and an even load distribution across a 2.79 mm (0.110 in.) line contact (the line length is less than the face width allowing for the face offset and the radius edge break). Typical dynamic tooth forces using the same rigs and gears of the same specification have been measured (ref. 15), and the results are provided in figure 3. The tooth forces reported in figure 3 are the dynamic forces normal to the tooth surface (or in other words tangent to the base circle) for a nominal pitch-line test load intensity of 580 N/mm (3,300 lb/in.). The static contact force (tangent to the base circle) used for stress calculations for such test load intensity was 1,720 N (387 lb). This value for the contact force is the value required for static torque equilibrium at the pitch-point, and it is somewhat less than the measured typical dynamic forces.

The fatigue tests ran continuously and unattended (24 hr/day). The test was stopped when the root-mean-squared acceleration level of the gearbox housing exceeded a limit. The gears were tested at 10,000 rpm, which gave a pitch-line velocity of 46.5 m/s (9,154 ft/min). If a gear pair operated for more than 500 hours (corresponding to 300 million stress cycles) without fatigue failure, the test was suspended.

The pitch line elastohydrodynamic (EHD) film thickness was calculated using the rectangular conjunction formula of Dowson and Higginson (ref. 16). For calculating the film thickness, it was assumed that the gear temperature was equal to the oil outlet temperature. The results of film thickness calculations and the values used for absolute viscosity and the pressure-viscosity coefficient are provided in table 4. The lubricant properties used for EHD calculations are extrapolations using measured values for kinematic viscosity and typical values for specific gravity and pressure-viscosity coefficients at the test temperature (table 4). Also provided in table 4 are specific film thickness (lambda ratio) values, calculated as the minimum film thickness divided by the initial specified composite surface roughness.

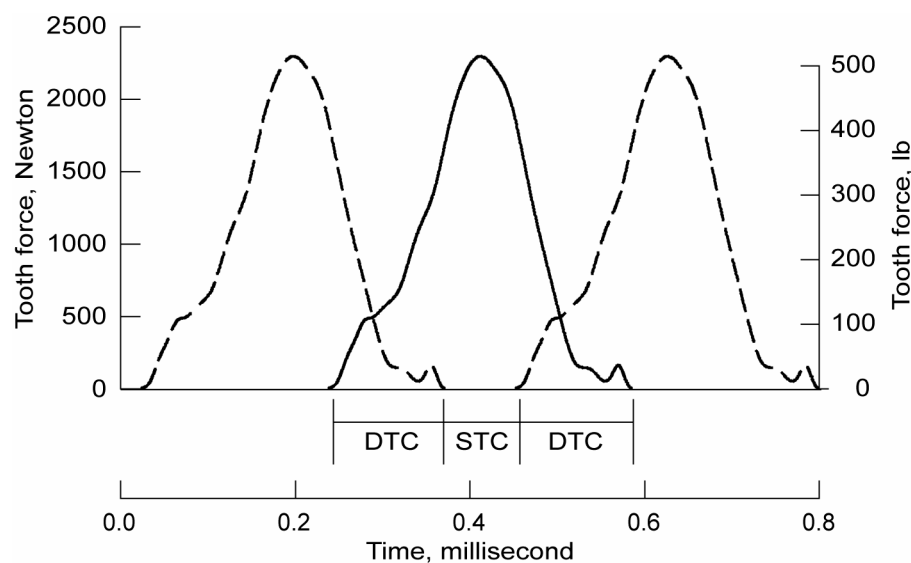


Figure 3.—Measured dynamic tooth force at nominal test conditions (ref. 15). The solid line is the measured data, and the dashed lines are replicates of the measured data spaced along the ordinate at the equivalent of one tooth pitch. The zones of double tooth contact (DTC) and single tooth contact (STC) are illustrated.

TABLE 4.—LUBRICANT PROPERTIES

Parameter	Lubricant						
	A	B	C	D	E	G	H
Kinematic viscosity, (cSt) at 311 K (100 °F) at 372 K (210 °F)	21.0 4.31	29.78 5.39	12.2 3.2	27.6 5.18	34.4 7.37	52.4 8.98	28.4 5.37
Flash point, K (°F) Pour point, K (°F)	516 (470) 200 (–100)	539 (510) 217 (–70)	489 (420) -----	544 (520) 211(–80)	519 (475) 214 (–75)	561 (550) 213 (–76)	525 (485) 217 (–70)
Specific gravity at 289 k (60 °F)	1.00	1.00	-----	0.995	0.947	0.986	0.990
Total acid number (tan) Mg Koh/g oil	0.07	0.03	0.15	0.40	0.06	1.01	0.09
Absolute viscosity, (N-s/m <sup>2</sup> ) at 348 K (167 °F) *	0.014	0.018	0.010	0.017	0.022	0.028	0.017
Pressure-viscosity coefficient, (m <sup>2</sup> /N) *	9.×10 <sup>–9</sup>	10.5×10 <sup>–9</sup>	7.5×10 <sup>–9</sup>	11.×10 <sup>–9</sup>	12.×10 <sup>–9</sup>	11.×10 <sup>–9</sup>	11.×10 <sup>–9</sup>
Film thickness, μm (μin) Lambda ratio **	0.40 (16) 0.69	0.52 (20) 0.90	0.28 (11) 0.49	0.51 (20) 0.89	0.65 (25) 1.12	0.73 (29) 1.26	0.51 (20) 0.89
Specification	None***	MIL-L-23699	MIL-L-7808J	DOD-L-85734	DERD-2478	None	DOD-L-85734

\* data used for film thickness calculations

\*\* Lambda ratio = calculated minimum film thickness/initial composite surface roughness

\*\*\* basestock oil

## 2.5 Measurement of Surface Profiles

A gear coordinate measurement machine is used in this study to quantify the wear depths. Figure 4 shows the inspection machine used in this study while inspecting one of the test specimens. Two types of inspections were performed here. The first type of inspection used was a standard inspection as used by

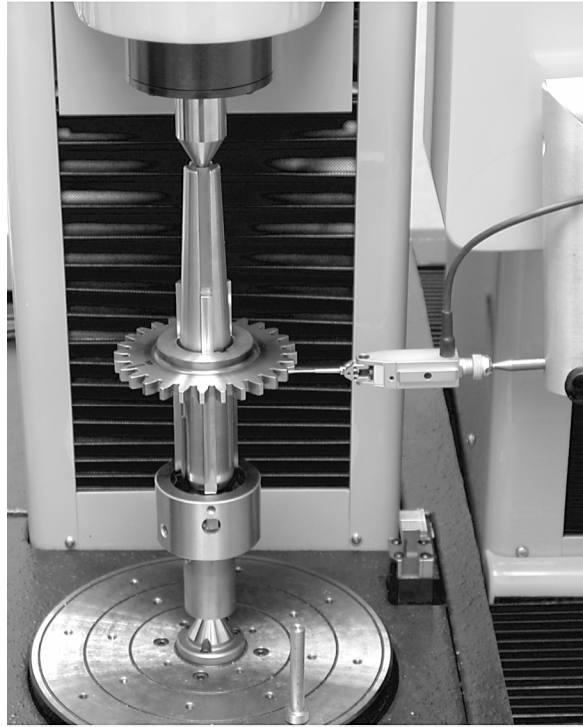


Figure 4.—A test gear while being inspected on the gear coordinate measurement machine.

the gear industry. These inspections include the measurements of lead traces (from one side to the other at given constant radii) and involute traces (from the root to the tip of a tooth at given constant lead locations). In figure 5, such inspections of a new test specimen are shown. Here, four teeth at nearly 90 degrees spacing were inspected. For each tooth inspected, two involute traces (traces A and B at one-third lead locations) and two lead traces (trace A in the addendum and trace B in the dedendum region) are shown in figure 5. It is evident from this figure that the profiles were machined very precisely with straight lead traces and a designed amount of tip relief. Figure 6 shows the lead charts for the teeth of a specimen at the end of its test. Since the actual contact occurred at the left portion of the face width only (due to face off-set described earlier), the section to the right represents the unworn original tooth surface and the large step down to the left represents wear. It is obvious here that the wear magnitudes are rather significant and can be quantified by comparing the worn surface location (left) to the unworn surface location (right). It is also clear, and typical, that the wear amount is much larger in dedendum region (traces B) than those in addendum region (traces A).

While standard inspections are useful to visualize the surface wear in any given direction (lead or involute), a large number of such traces are required to determine the maximum wear depth. For this purpose, the three-dimensional (3-D) topographical gear inspection method developed by Bajpai, et al. (ref. 10) was employed. When this method was applied to all the teeth of a test specimen, it was commonly observed that the maximum wear depth varies from tooth to tooth. In figure 7, a worn specimen that has a significant variation of maximum wear depths from tooth to tooth is shown. Here, a sinusoidal distribution of wear is evident. The maximum wear amount on tooth 27 is nearly zero while tooth 13 has nearly 160  $\mu\text{m}$  maximum wear. Figure 8 shows the 3-D topographical inspections of four teeth of the same gear. Most of the gears had a more uniform wear distribution than shown by this extreme example illustrated in figures 7 and 8. Measuring the maximum wear amounts on all the teeth on all gears was considered as excessively time consuming and hence not practical. In order to be able to represent the wear amount of a given gear by a single number, an average maximum wear parameter was defined as  $h = \frac{1}{4}(h_1 + h_8 + h_{15} + h_{22})$ . In other words, the wear values of four equally spaced teeth (1, 8,

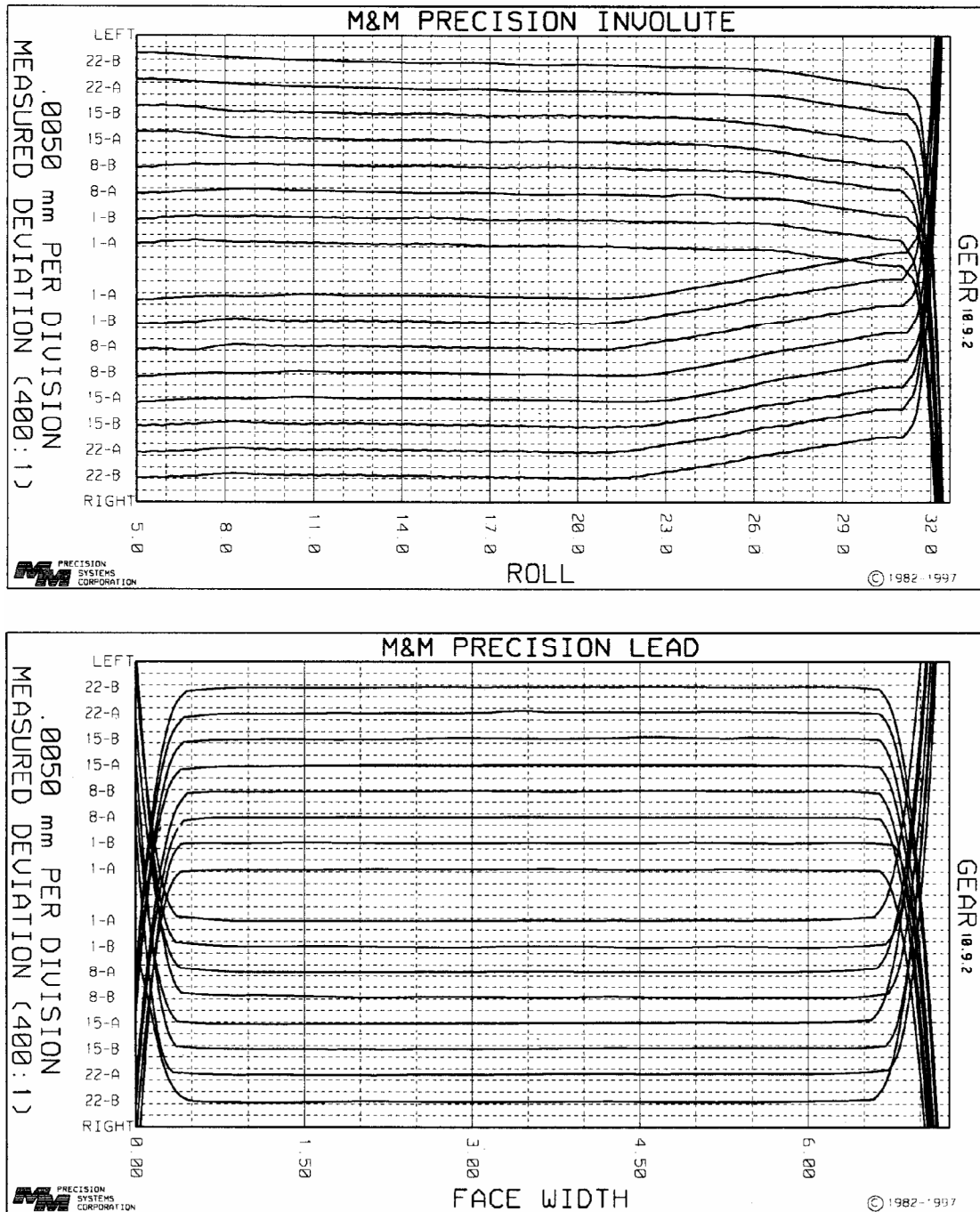


Figure 5.—Involute and lead inspection charts of a typical new gear pair. Two lead and involute traces of both sides of teeth 1, 8, 15 and 22 are shown.

15, and 22) were used to define  $h$ . From the average maximum wear parameter  $h$ , the wear rate was defined as  $\bar{h} = h/C$  where  $C$  is the recorded number of revolutions of the gear pair in millions (or millions of meshing cycles). For the majority of specimens, the value of  $C$  is equal to the measured surface fatigue life for the particular gear pair. For some specimens,  $C$  is the number of cycles completed without surface fatigue (the fatigue testing procedure made use of a nominal 300 million cycle limit to reduce the total test time for the fatigue life evaluations).

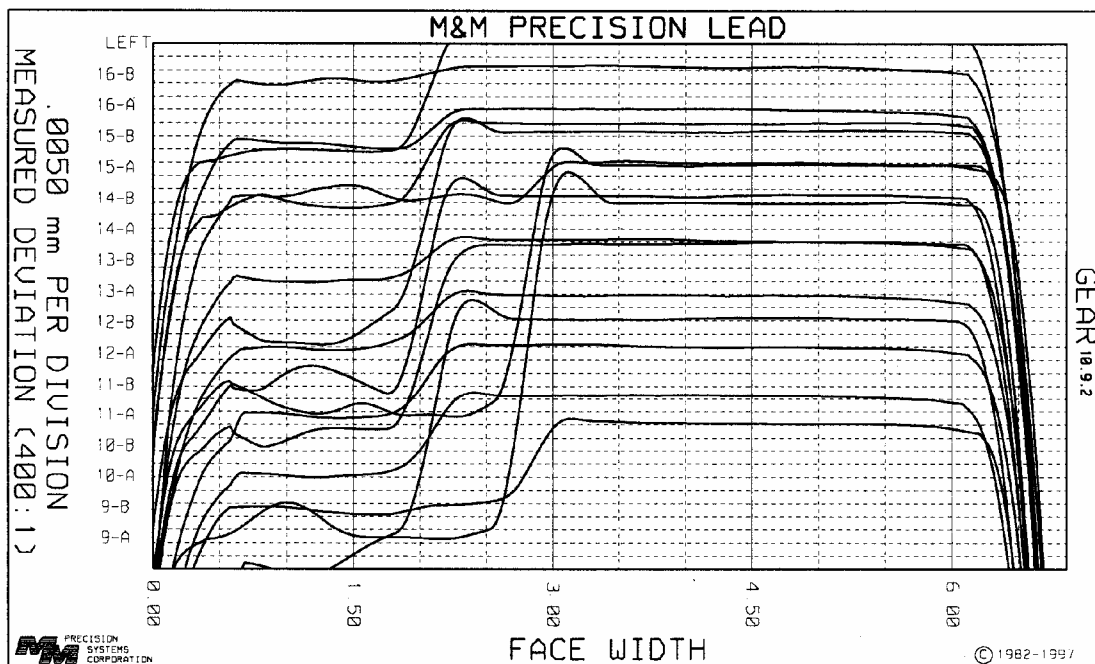


Figure 6.—A lead inspection chart of an example test specimen after the test was completed. Two traces of teeth 9 to 16 are shown. Only the face width plotted as (approximately) 0.00 to 3.00 mm was tested. Traces “A” are in the addendum, traces “B” in the dedendum.

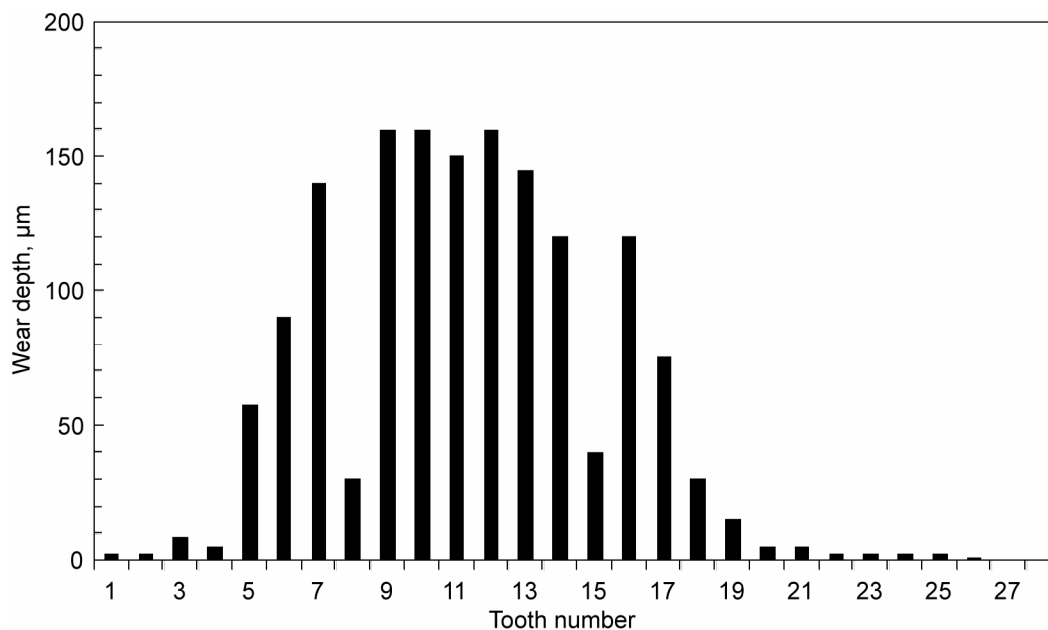


Figure 7.—Variation of maximum wear depth of an example test gear as a function of tooth number.

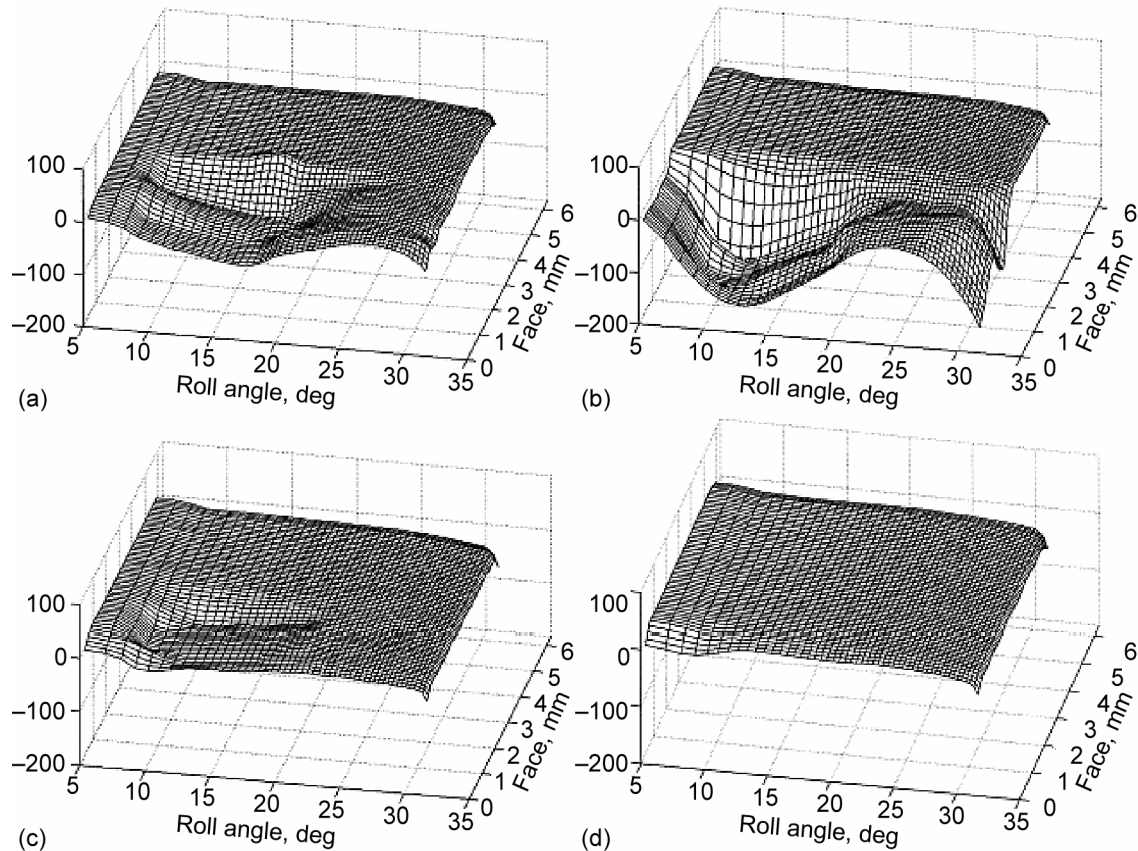


Figure 8.—High-resolution 3D CMM inspections showing deviation surface profiles from perfect involute, units of  $\mu\text{m}$ , for (a) tooth 6, (b) tooth 12, (c) tooth 19 and (d) tooth 26 of the same gear shown in Fig. 10.

### 3. Test Lubricants

The lubricants used had been selected to study the effects of lubricants with similar base stocks but differing viscosities on the surface fatigue lives of AISI 9310 spur gears. Fatigue data were reported for seven lubricants (ref. 13) that were identified as lubricants A through G. For tests using lubricant F, there were insufficient numbers of tested gears available for wear measurements, and so lubricant F was not included as part of the present study. Subsequent to the publication of reference 13, Townsend and Shimski conducted additional tests using other lubricants. Although these fatigue data have not yet been published, the test results, records, and some of the specimens were available to the present investigators. For the present wear study, gear specimens tested using a lubricant designated as H in this article were analyzed for wear.

Properties of the lubricants studied are provided in table 4, and descriptions of the lubricants follow. Lubricant A is an unformulated base stock lubricant with no additives, and it has a viscosity in between that required for the MIL-L-7808J and MIL-L-23699 specifications. Lubricant B is a 5 cSt lubricant meeting the MIL-L-23699 specification, and it has a small amount of boundary lubrication additive. Lubricant C is a 3 cSt lubricant meeting the MIL-L-7808J specification. Lubricant C has the lowest viscosity of all the lubricants included in the study, and it has a proprietary extreme pressure additive package. Lubricants D and H are lubricants developed for helicopter gearboxes, and both lubricants meet the DOD-L-85734 specification. Lubricants D and H are 5 cSt lubricants with extreme pressure additive packages, and these two lubricants were obtained from two different manufacturers. Lubricant E is a 7.5 cSt lubricant with an extreme pressure additive, and this lubricant meets the development

specification DERD-2487. Lubricant G is a 9 cSt base stock industrial grade lubricant. Six of the seven lubricants included in this study could be classified as synthetic polyol-ester base stock lubricants. Lubricant E is a polyalkylene-glycol base stock with a small amount of boundary lubricant additive.

## 4. Results and Discussion

### 4.1 Amounts and Descriptions of Wear

A total of 112 gear specimens were inspected using a gear coordinate measuring machine to evaluate the average wear depth and wear rate using the methodology described in section 2.5. The number of samples for each lubricant test population was dependent on the availability of the test specimens. Gears tested with lubricant C had the lowest number of samples,  $N = 8$ , and gears tested with lubricant H had the largest number of samples,  $N = 23$ . Four teeth on each gear specimen were inspected (a total of 448 teeth), and wear amounts were averaged to determine the average wear rate for each gear. Table 5 summarizes the measured wear amounts and wear rates (mean and standard deviation values) and the sample sizes for each lubricant. The amount of scatter of the wear data from gear specimen to specimen is quite significant. The distribution of wear rates is illustrated in figure 9. From table 5 and figure 9, it is clear that lubricant C resulted in the most severe wear rates while lubricant G performed the best. Other lubricants resulted in levels of wear between these extremes.

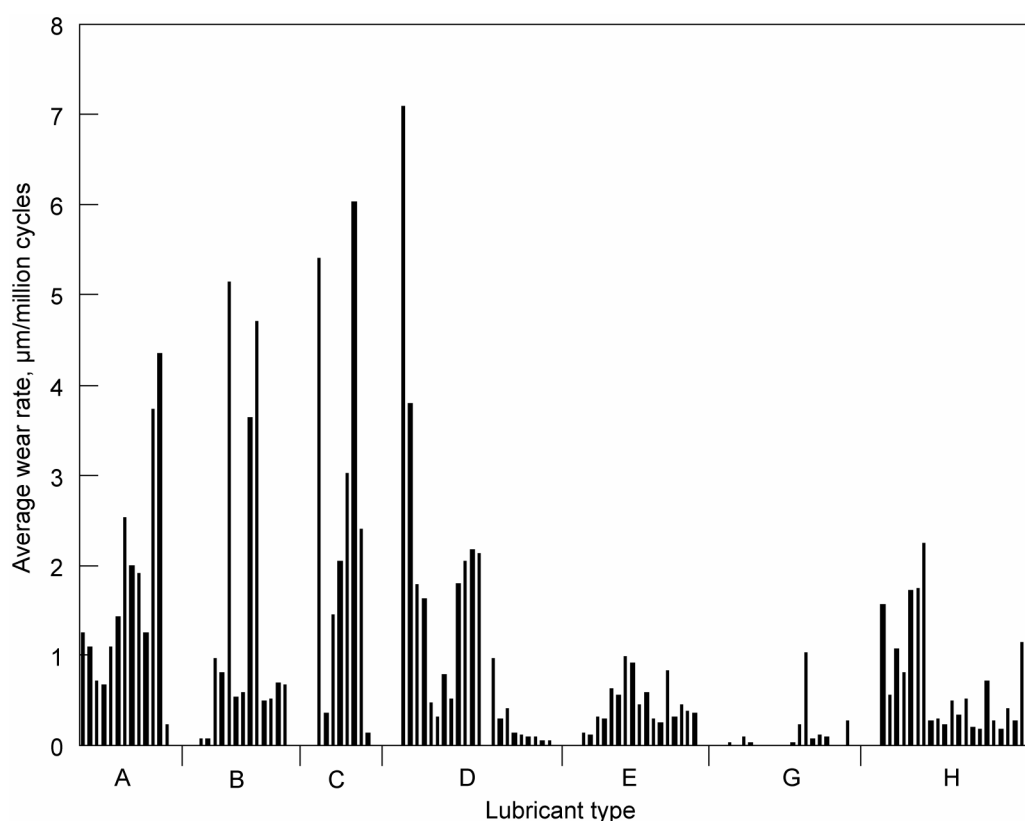


Figure 9.—Summary of the measured average wear rates as a function of lubricant type.



TABLE 5.—WEAR AMOUNT,  $h$  AND WEAR RATE,  $\bar{h}$  PARAMETERS FOR THE SEVEN TEST LUBRICANTS.

Lubricant	Wear amounts, $h$ ( $\mu\text{m}$ )		Wear rates, $\bar{h}$ ( $\mu\text{m}/\text{million cycles}$ )		Sample size
	Mean	Std. dev.	Mean	Std. dev.	
A	66	19	1.7	1.2	13
B	73	55	1.4	1.8	13
C	79	62	2.6	2.2	8
D	49	38	1.2	1.6	20
E	55	30	0.46	0.3	17
G	8.1	13	0.11	0.2	18
H	66	70	0.61	0.6	23

To help document and characterize the wear, photos of worn gear teeth, one for each lubricant tested, are provided in figure 10. In general, the wear can be described as a mild, polishing wear over most of the tooth profile. Near the start and end of contact, there exists some evidence of abrasive and/or light adhesive wear (scoring-like marks). In general, the scoring-like marks that appeared at the positions of high sliding tended to be less severe for lubricants with higher viscosities. It is evident that lesser wear amounts occurred near the pitch line where sliding velocities are small as compared to the roots and tips of the teeth. The worn surfaces in some cases were remarkable in that worn and very smooth regions can be found a slight distance from the pitch point while the grinding patterns were still visible at the

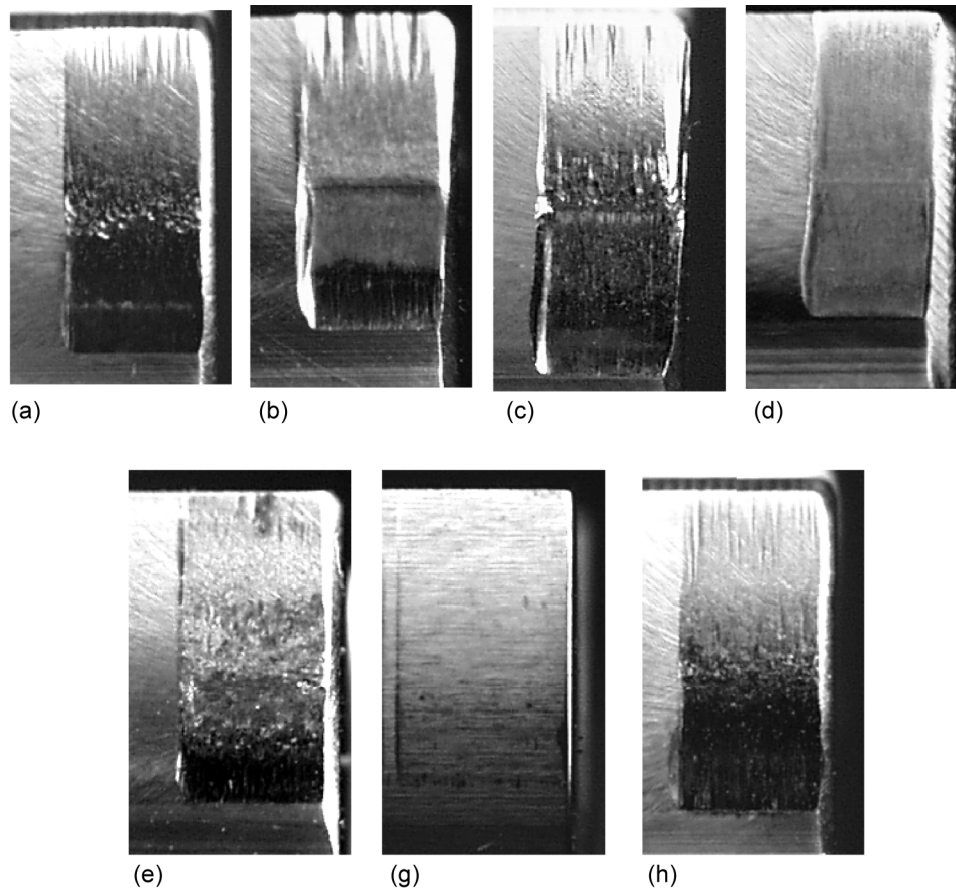


Figure 10.—Worn surfaces of the test gears for each of seven lubricants. (a) Lubricant A. (b) Lubricant B. (c) Lubricant C. (d) Lubricant D. (e) Lubricant E. (g) Lubricant G. (h) Lubricant H.

pitch point. The photograph for the tooth tested with lubricant G demonstrates that for this lubricant and for the chosen test conditions, the working surfaces were well protected with few direct asperity contacts and, for practical purposes, nearly zero wear.

The maximum wear depths invariably occurred in the dedendum region of the teeth, that is somewhat below the pitch-line. In the regions of maximum wear depth, the worn surfaces have a worked and polished appearance. Any scratching marks in the direction of sliding that were present in this region of maximum wear can be characterized as minor scratching consistent with abrasive wear. There was no evidence of destructive scoring (scuffing), spalling, pitting, nor micropitting (grey-staining) failures on the teeth selected for wear measurements. Some teeth on the gears had surface fatigue damage (the intent of the original study (ref. 13)), but care was taken to select teeth without such damage for measurements of wear. Illustrations of teeth with surface fatigue damage for these tests were provided by Townsend and Shimski (ref. 13).

## 4.2 Influence of Lubricant Type on Gear Wear

To characterize differences in wear owing to different lubricants, wear rates are plotted as a function of key lubrication parameters. Figure 11 shows  $\bar{h}$  as a function of the absolute viscosity of the lubricants at the testing temperature as listed in table 4. It is clear from this figure that the wear rates are an inverse function of the viscosity of the lubricant. Lubricant C has the lowest viscosity ( $0.010 \text{ N-s/m}^2$ ) resulting in the most severe wear rate of nearly  $2.6 \mu\text{m}$  per million cycles while lubricant G with the highest viscosity value ( $0.028 \text{ N-s/m}^2$ ) resulted in the lowest wear rate of about  $0.11 \mu\text{m}$  per million cycles. The other lubricants generally are ordered in sequence relative to their viscosity values. From figure 11, the lubricants B, D, and H have differing wear rates but similar viscosity values. It is perhaps significant that lubricant B meets the specification MIL-L-23699 (turbine engine lubricants) while lubricants D and H meet the specification DOD-L-85734 (helicopter transmission lubricants). One might expect lubricants D and H developed for gearing to perform better than lubricant B in a gear test. This scatter in the wear results for lubricant B, D, and H (in spite of nearly equal viscosities) highlights that lubricant composition and additive packages along with viscosity strongly influence the lubricant's capability for wear protection.

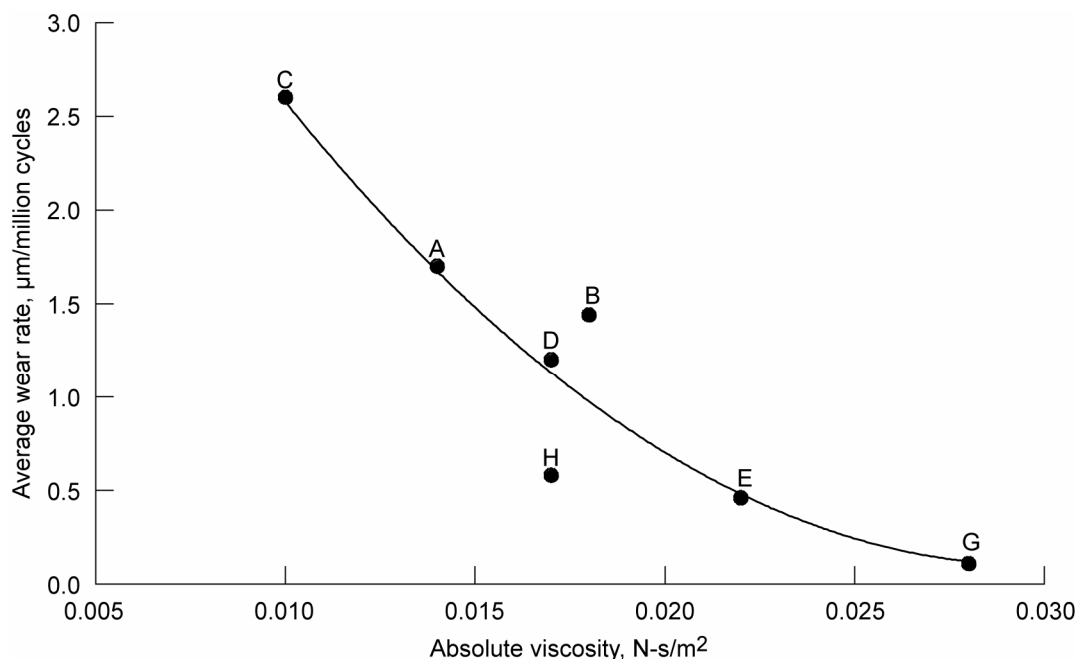


Figure 11.—Variation of average wear rate as a function of viscosity at the testing temperature for each lubricant. The solid line is a trend line representing a quadratic curve fit.

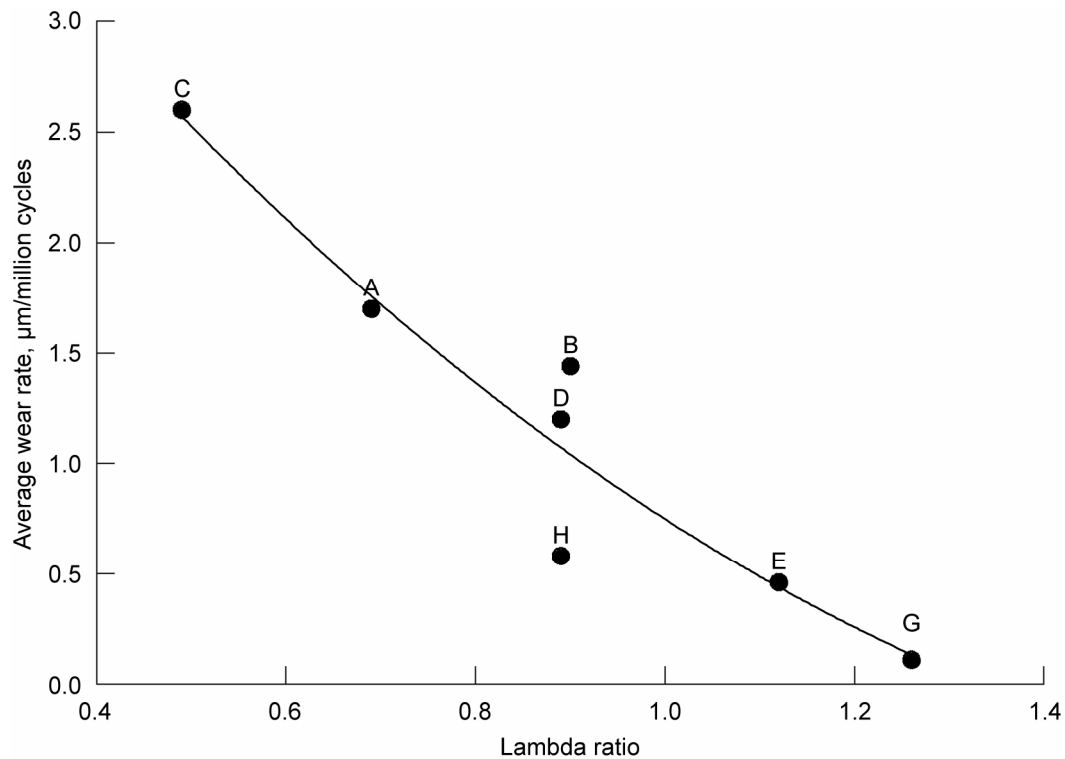


Figure 12.—Variation of average wear rate as a function of lambda ratio. The solid line is a trend line representing a quadratic curve fit.

A very similar behavior is observed when  $\bar{h}$  is plotted as a function of the lambda ratio that is defined as the ratio of central film thickness (determined by using the smooth surface EHL formulas of Dowson and Higginson (ref. 16)) to the initial specified composite surface roughness of mating gear surfaces. The specified root-mean-square roughness of  $0.4 \mu\text{m}$  results in a composite roughness of about  $0.57 \mu\text{m}$ . In figure 12, the relative ranking of the test lubricants for their wear performance remain inversely proportional to the lambda ratio (the same order as fig. 11). The lubricant C having the lowest viscosity results in a very thin film and a very low lambda ratio (about 0.49) as listed in table 4. As a result, mixed lubrication conditions with significant asperity interactions occurred along with extensive wear. The opposite is true for lubricant G that allows a relatively large lambda ratio of 1.26 minimizing the amount of surface wear. Other lubricants are ordered between these two extremes depending on the lambda ratio.

#### 4.2 Wear versus Contact Fatigue Life

The gear fatigue experiments that were conducted by Townsend and Shimski (ref. 13) established and quantified the influence of lubricant viscosity on gear surface fatigue lives. The surface fatigue life results are summarized in table 6. The table is sorted by the measured 10 and 50 percent lives. These percentile life estimates were determined by modeling the life dispersions as Weibull distributions and employing the regression methods of Johnson (ref. 17) to determine the values for the Weibull slope and scale parameters. In figure 13, estimated 10- and 50-percent surface fatigue lives corresponding to each lubricant are plotted against the viscosity of the lubricant. The results demonstrate that, in general, the greater the viscosity of the lubricant the longer the surface fatigue lives. The solid lines in figure 13 represents exponential relationships observed as linear lines since the surface fatigue lives are displayed using a log scale.

TABLE 6.—SURFACE FATIGUE TEST RESULTS (REF. 13)

Lubricant code	Lubricant basestock	Gear System lives, millions of cycles		Weibull slope	Failure index	Lubricant viscosity (cSt) at 372 °K (210 °F)
		10 percent	50 percent			
A	polyol-ester	5.1	20	1.4	30/30	4.3
C	polyol-ester	5.7	21	1.5	20/20	3.2
D	polyol-ester	12	51	1.3	17/20	5.2
B	polyol-ester	12	76	1.0	20/20	5.4
H	polyol-ester	35	79	1.6	19/24	5.4
E	polyalkylene-glycol	47	152	1.6	15/19	7.4
G	polyol-ester	103	568	1.1	5/18	9.0

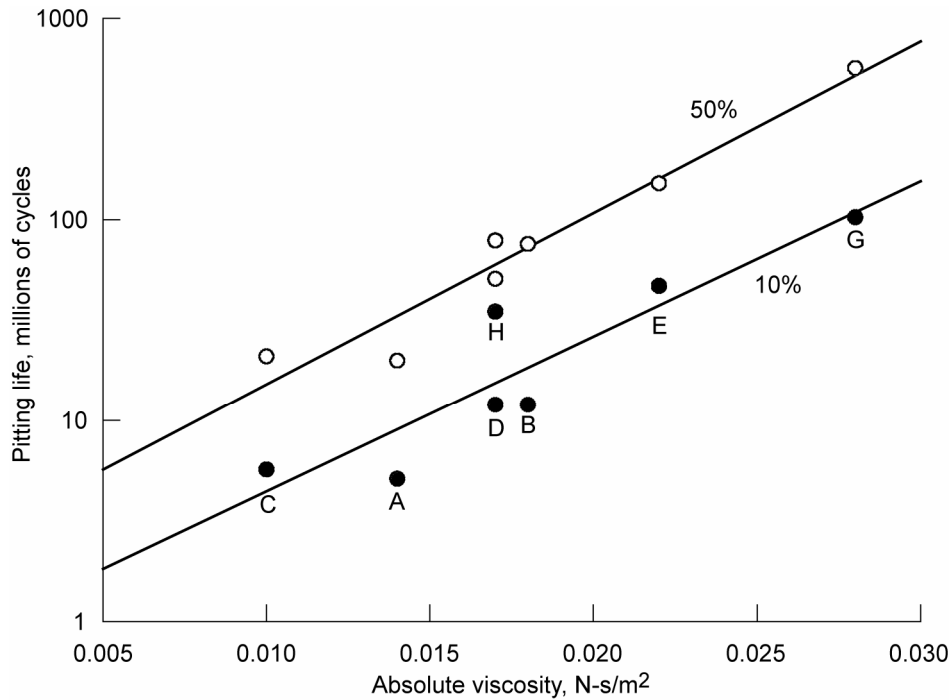


Figure 13.—Variation of surface fatigue life as a function of viscosity of each lubricant. The solid lines are trends representing exponential curve fits at 10% population failed and 50% population failed.

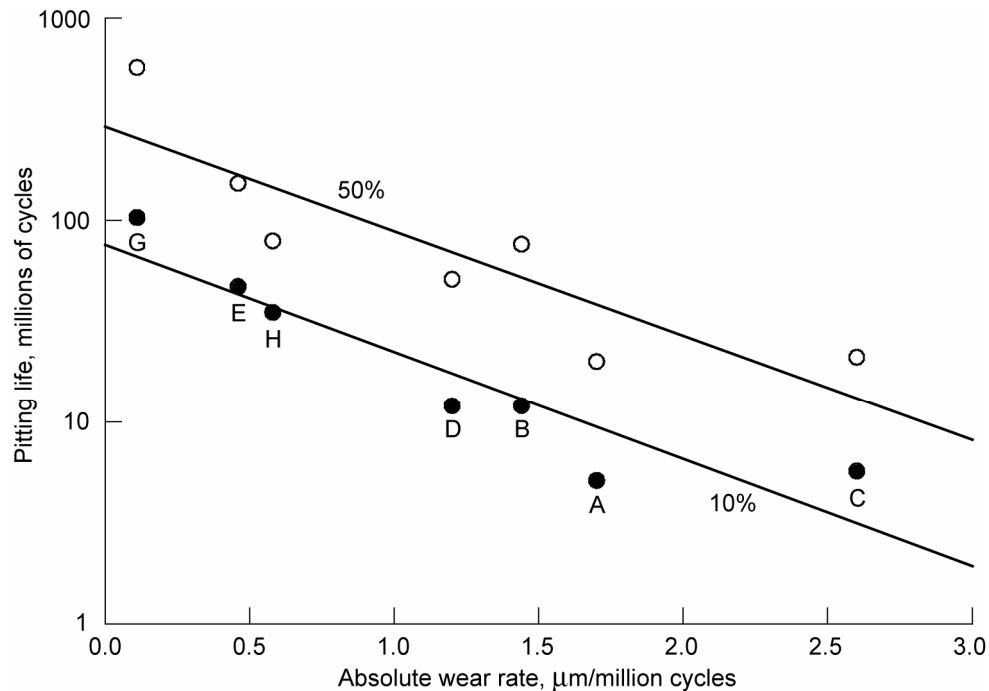


Figure 14.—The relationship between surface fatigue life and average wear rate. The solid lines are trends representing exponential curve fits at 10% population failed and 50% population failed.

From figures 13 and 14, it is evident that the lubricant viscosity has a similar trend for both surface fatigue life and wear. For the lubricants tested here, the larger the viscosity of the lubricant the longer the fatigue lives and smaller the wear amounts. In figure 14, the fatigue lives and wear rates for each lubricant group are plotted to show the correlation. The relationship between the wear rates and surface fatigue lives is exponential. This correlation highlights the dominant role of the lubricant viscosity. The relationship depicted in figure 14 shows that a lubricant that functioned well in terms of surface fatigue life also tended to function well in terms of wear. Likewise, it can be stated that very low wear rates indicates a relatively favorable lubrication condition that also tended to promote long surface fatigue life. Lastly, lubricants with nearly equal viscosity but differing additives offer differing levels of protection for wear and surface fatigue.

## 5. Conclusion

In this study, the influence of lubricant viscosity and additives on the wear rate of spur gear pairs was investigated experimentally. The gear specimens from a comprehensive gear durability test program that includes seven different lubricants were inspected to demonstrate the influence of the lubrication condition on gear tooth surface wear. The results indicate that the wear rates are strongly related to the viscosity of the lubricant. Lubricants with larger viscosity result in larger lambda ratios and lower wear rates. A similar strong influence of the lubricant viscosity was previously observed for surface fatigue lives as well. An exponential relationship between the surface fatigue lives and the average wear rates was found. The data suggest that viscosity plays a dominant role. There were also considerable differences in wear amounts for three lubricants with differing additive packages but similar compositions and viscosities.

## References

1. Choy, F.K., Polyshchuk, V. and Zakrajsek, J.J., Handschuh, R.F. and Townsend, D.P., 1996, "Analysis of the Effects of Surface Pitting and Wear on the Vibration of a Gear Transmission System," *Tribology International*, 29, 77–83.
2. Mackaldener, M. Flodin, A. and Andersson, S., 2001, "Robust Noise Characteristics of Gears Due to their Applications, Manufacturing Errors and Wear," JSME International Conference on Motion and Power Transmission, MPT 2001, Fukuoka, Japan, 21–26.
3. Kuang, J.H. and Lin, A.D., 2001, "The Effect of Tooth Wear on the Vibration Spectrum of a Spur Gear Pair," *ASME Journal of Vibration and Acoustics*, 123, 311–317.
4. Chen, Y. and Matubara, M., 2001, "Effect of Automatic Transmission Fluid on Pitting Fatigue Strength of Carburized Gears," JSME International Conference on Motion and Power Transmission, MPT 2001, Fukuoka, Japan, 151–156.
5. Cioc, C., Cioc, S., Kahraman, A. and Keith, T.G., 2002, "A Deterministic Elastohydrodynamic Lubrication Model of High-Speed Transmission Components," *Tribology Transactions*, 45, 556–562.
6. Shifeng, W. and Cheng, H.S., 1993, "Sliding Wear Calculation in Spur Gears," *Journal of Tribology*, 115, 493–503.
7. Flodin, A. and Andersson, S., 1997, "Simulation of Mild Wear in Spur Gears," *Wear*, 207, 123–128.
8. Flodin, A. and Andersson, S., 2000, "Simulation of Mild Wear in Helical Gears," *Wear*, 241, 123–128.
9. Flodin, A. and Andersson, S., 2001, "A Simplified Model for Wear Prediction in Helical Gears," *Wear*, 249, 285–292.
10. Bajpai, P., Kahraman, A., and Anderson, N., 2003, "Development of Surface Wear Model for Helical Gear Pairs," In review, *ASME Journal of Tribology*.
11. Archard, J.F., 1953, "Contact of Rubbing Flat Surfaces," *Journal of Applied Physics*, 24, 981–988.
12. Challen, J.M. and Oxley P.L.B., 1986, "Prediction of Archard's Wear Coefficient for Sliding Metallic Sliding Friction Assuming Low Cycle Fatigue Wear Mechanism," *Wear*, 111, 275–288.
13. Townsend, D.P., and Shimski, J., 1994, "Evaluation of the EHL Film Thickness and Extreme Pressure Additives on Gear Surface Fatigue," NASA TM-106663.
14. Townsend, D.P., Chevalier, J.L., and Zaretsky, E.V., 1973, "Pitting Fatigue Characteristics of AISI M-50 and Super Nitralloy Spur Gears," NASA TN D-7261.
15. Krantz, T.L., 2002, "The Influence of Roughness on Gear Surface Fatigue," Ph.D. Thesis, Case Western Reserve University, Cleveland, Ohio.
16. Dowson, D. and Higginson, G., 1966, *Elasto-Hydrodynamic Lubrication*, Pergamon Press.
17. Johnson, L., 1964, *The Statistical Treatment of Fatigue Experiments*, Elsevier, New York, NY.

REPORT DOCUMENTATION PAGE			Form Approved OMB No. 0704-0188	
Public reporting burden for this collection of information is estimated to average 1 hour per response, including the time for reviewing instructions, searching existing data sources, gathering and maintaining the data needed, and completing and reviewing the collection of information. Send comments regarding this burden estimate or any other aspect of this collection of information, including suggestions for reducing this burden, to Washington Headquarters Services, Directorate for Information Operations and Reports, 1215 Jefferson Davis Highway, Suite 1204, Arlington, VA 22202-4302, and to the Office of Management and Budget, Paperwork Reduction Project (0704-0188), Washington, DC 20503.				
1. AGENCY USE ONLY (Leave blank)		2. REPORT DATE October 2005	3. REPORT TYPE AND DATES COVERED Technical Memorandum	
4. TITLE AND SUBTITLE  An Experimental Investigation of the Influence of the Lubricant Viscosity and Additives on Gear Wear			5. FUNDING NUMBERS  WBS-22-714-09-16 1L161102AF20	
6. AUTHOR(S)  Timothy L. Krantz and Ahmet Kahraman				
7. PERFORMING ORGANIZATION NAME(S) AND ADDRESS(ES)  National Aeronautics and Space Administration John H. Glenn Research Center at Lewis Field Cleveland, Ohio 44135-3191			8. PERFORMING ORGANIZATION REPORT NUMBER  E-15272	
9. SPONSORING/MONITORING AGENCY NAME(S) AND ADDRESS(ES)  National Aeronautics and Space Administration Washington, DC 20546-0001 and U.S. Army Research Laboratory Adelphi, Maryland 20783-1145			10. SPONSORING/MONITORING AGENCY REPORT NUMBER  NASA TM-2005-213956 ARL-TR-3126	
11. SUPPLEMENTARY NOTES  Timothy L. Krantz, U.S. Army Research Laboratory, NASA Glenn Research Center; and Ahmet Kahraman, The Ohio State University, 190 N. Oval Mall, Columbus, Ohio 43210. Responsible person, Timothy L. Krantz, organization code RSM, 216-433-3580.				
12a. DISTRIBUTION/AVAILABILITY STATEMENT  Unclassified - Unlimited Subject Category: 37  Available electronically at <a href="http://gltrs.grc.nasa.gov">http://gltrs.grc.nasa.gov</a> This publication is available from the NASA Center for AeroSpace Information, 301-621-0390.			12b. DISTRIBUTION CODE	
13. ABSTRACT (Maximum 200 words)  The influence of lubricant viscosity and additives on the average wear rate of spur gear pairs was investigated experimentally. The gear specimens of a comprehensive gear durability test program that made use of seven lubricants covering a range of viscosities were examined to measure gear tooth wear. The measured wear was related to the as-manufactured surface roughness, the elastohydrodynamic film thickness, and the experimentally determined contact fatigue lives of the same specimens. In general, the wear rate was found to be inversely proportional to the viscosity of the lubricant and to the lambda ratio (also sometimes called the specific film thickness). The data also show an exponential trend between the average wear rates and the surface fatigue lives. Lubricants with similar viscosities but differing additives and compositions had somewhat differing gear surface fatigue lives and wear rates.				
14. SUBJECT TERMS  Gear; Wear; Lubrication; Elastodynamics			15. NUMBER OF PAGES 24	
			16. PRICE CODE	
17. SECURITY CLASSIFICATION OF REPORT  Unclassified	18. SECURITY CLASSIFICATION OF THIS PAGE  Unclassified	19. SECURITY CLASSIFICATION OF ABSTRACT  Unclassified	20. LIMITATION OF ABSTRACT	





